



Original article

Design and synthesis of 2-styryl of 5-Nitroimidazole derivatives and antimicrobial activities as FabH inhibitors



Yong-Tao Duan¹, Zhong-Chang Wang¹, Ya-Li Sang, Xiang-Xiang Tao, Shashikant B. Teraiya, Peng-Fei Wang, Qing Wen, Xiao-Jing Zhou, Liang Ding, Yong-Hua Yang*, Hai-Liang Zhu*

State Key Laboratory of Pharmaceutical Biotechnology, Nanjing University, Nanjing 210093, People's Republic of China

ARTICLE INFO

Article history:

Received 21 April 2013

Received in revised form

7 January 2014

Accepted 5 February 2014

Available online 15 February 2014

Keywords:

5-Nitroimidazole

FabH inhibitors

Antibacterial activities

Cytotoxicity

ABSTRACT

A series of 2-Styryl-5-Nitroimidazole derivatives (**25–48**) have been synthesized and their biological activities were also evaluated against two Gram-negative bacterial strains: *Escherichia coli* and *Pseudomonas aeruginosa* and two Gram-positive bacterial strains: *Bacillus subtilis* and *Bacillus thuringiensis* as potential FabH inhibitors. All the compounds were structurally determined by ¹H NMR, MS, and elemental analysis. *E. coli* β -ketoacyl-acyl carrier protein synthase III inhibitory assay and docking simulation indicated that compound **33** with IC₅₀ of 9.0–36.4 μ g/mL and compound **47** with IC₅₀ of 6.3–34.3 μ g/mL against bacterial strains were most potent inhibitors of *E. coli* FabH. And more, compounds **33** and **47** which possessed a broad-spectrum of antibacterial activities didn't exhibit any toxicity towards macrophage.

© 2014 Elsevier Masson SAS. All rights reserved.

1. Introduction

Infections due to bacteria such as *Escherichia coli* have been major cause of human morbidity and mortality [1,2]. Although the innovative research for antibiotics has improved mankind's health status by confining life threatening infections, the emergence and spread of bacterial resistance represents a severe global problem [3,4], and resistance against causal organisms has been reported and development of agents targeted at these organisms pose a challenge presently [5,6]. Therefore, the development of new types of antibacterial agents is a very important task.

In recent years, much of the research effort is oriented to the design of new antibacterial agents with high efficiency [7–12]. One of the most attractive biochemical pathways to be used as the target for new antibacterial agents is the fatty acid biosynthesis (FAB). This pathway has been demonstrated to be essential for bacteria cell survival [13,14]. Fatty acid biosynthesis (FAB) is an essential metabolic process for prokaryotic organisms and is required for cell viability and growth [15]. β -ketoacyl-acyl carrier protein (ACP) synthase III, also known as FabH or KAS III, plays an essential and regulatory role in bacterial FAB [16,17]. In spite of the denil necessity of FabB and FabF for Gram-positive bacteria, the key

role and ubiquitous structure of FabH have guaranteed that FabH inhibitors are potent antibiotics with broad-spectrum activity. Importantly, the residues that comprise the active site are essentially invariant in various bacterial FabH molecules [18]. And more, our previous research also suggests that FabH can be used as an effective molecular target for the development of new antibacterial agents.

Presently, infection is primarily treated by instituting antimicrobials therapy. Antimicrobial drugs such as metronidazole, secnidazole kill microbes in host tissue and organs [19]. Particularly metronidazole is the most preferred treatment choice as 90% of patients respond to the therapy and has been widely used as an antimicrobial medicine [20]. However, resistances to metronidazole in many pathogenic bacteria as well as several side effects are also documented [21]. Therefore it is desirable to search for metronidazole derivatives or new lead compounds.

Our earlier investigations have provided evidence of the antibacterial properties of nitroimidazole derivatives, which support the idea that FabH can be used as an effective molecular target for nitroimidazole derivatives [8,22,23]. Some metronidazole derivatives have been predicted as notable radiosensitizers, anti-protozoal and antibacterial or antiepileptic agents [24]. However, to our knowledge, few reports have been dedicated to the synthesis and FabH inhibitory activity of compounds of modifications in the 2-position of the imidazole ring. Prior studies suggest that the 2-position modified 5-nitroimidazole drugs can overcome metronidazole resistance [25,26], and they raised the possibility that

* Corresponding authors.

E-mail address: zhuhl@nju.edu.cn (H.-L. Zhu).

¹ These two authors equally contributed to this paper.

metronidazole derivatives substituted in the 2-methyl group may be promising for developing new, potent, and safe drugs. Now it is clear that hydroxy and nitro group of metronidazole play a key role in the metabolic activation [27]. Thus, the structure modification at the pendant methyl group (2-position) of metronidazole has received our attention and then we designed and synthesized a library of substituted 2-styryl 5-nitroimidazole derivatives.

Herein, we describe the synthesis and structure–activity relationship (SAR) of a series of 2-styryl 5-nitroimidazole derivatives, and present their *in vitro* antibacterial activity against *Escherichia coli* (*E. coli*), *Bacillus thuringiensis* (*B. thuringiensis*), *Bacillus subtilis* (*B. subtilis*) and *Pseudomonas aeruginosa* (*P. aeruginosa*). Docking simulations are performed using the X-ray crystallographic structure of the FabH in complex with an inhibitor to explore the binding modes of these compounds at the active site. And more, to test the toxicity of compounds **33** and **47** against human macrophages, a research of cytotoxicity has been made.

2. Results and discussion

2.1. Chemistry

Twenty four 2-styryl 5-nitroimidazole derivatives were synthesized by the reaction of metronidazole with different substituted benzaldehyde in DMSO by adding rapidly a stirred solution of sodium methoxide in methanol at room temperature (Scheme 1). The refined compounds were finally obtained by subsequent purification with recrystallization. The chemical structures of these metronidazole derivatives were summarized in Table 1. These compounds gave satisfactory elementary analyses ($\pm 0.4\%$). ^1H NMR and ESI MS spectra data was consistent with the assigned structures. Among these compounds **28**, **30**, **33**, **35**, **37**, **40**–**45** and **47** were reported for the first time.

Furthermore, the crystal structure of compounds **35** and **37** was determined by single crystal X-ray diffraction analysis in Figs. 1 and 2, and their crystal data, data collection and refinement parameters for the compound **35** and **37** were listed in Table 2.

2.2. Biological activity

2.2.1. Antimicrobial activity

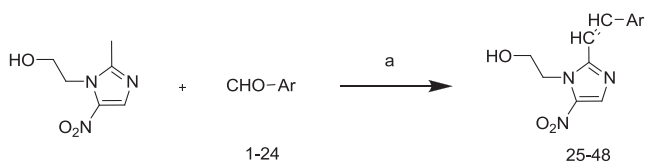
All the synthesized compounds (**25**–**48**) were screened for their antibacterial activities against two Gram-negative bacterial strains: *E. coli* and *P. aeruginosa* and two Gram-positive bacterial strains: *B. subtilis* and *B. thuringiensis* by MTT method. The IC_{50} of the compounds against these bacteria were presented in Table 3. Also included was the activity of reference compound Kanamycin and Penicillamine under identical conditions for comparison. The results revealed that most of the synthesized compounds exhibited significant antibacterial activities.

For most of the studied compounds, various substituents such as halogen, methyl, methoxyl and nitro group led to distinct

Table 1
Structures of compounds **25**–**48**.

Compound	Ar	Compound	Ar
25		37	
26		38	
27		39	
28		40	
29		41	
30		42	
31		43	
32		44	
33		45	
34		46	
35		47	
36		48	

antibacterial activities which always show more potent inhibitory activity against *E. coli* than compounds **25** and **46** with a bare aromatic ring (phenyl ring and naphthalene ring respectively), also we can see that the antibacterial activities were inferior than positive control Kanamycin and Penicillamine. However, compounds **33** and **47**, whose IC_{50} value were 36.4 and 34.3 $\mu\text{g}/\text{mL}$, displayed superior activity to the positive control Kanamycin with corresponding IC_{50} of 47.3 $\mu\text{g}/\text{mL}$ and Penicillamine with corresponding IC_{50} of 42.3 $\mu\text{g}/\text{mL}$. Addition of larger side chains at the phenyl



^a Reagents and conditions: Sodium methoxide, DMSO, methanol, room temperature;

Scheme 1.

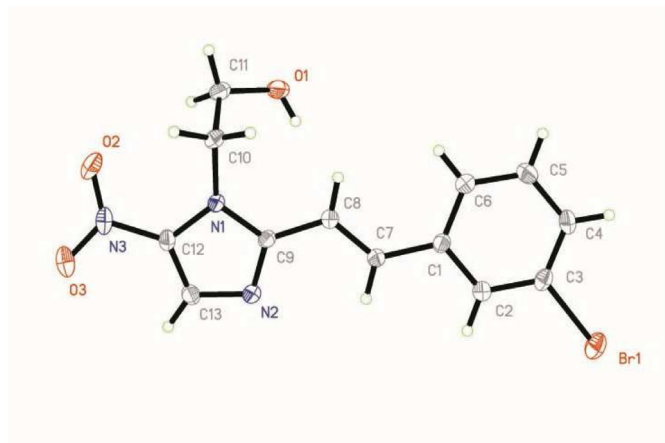


Fig. 1. Crystal structure diagram of compound **35**. H atoms are shown as small spheres of arbitrary radii.

moiety, including $\text{CH}_2(\text{OC}_2\text{H}_5)_2$ (**36**) and $\text{N}(\text{CH}_3)_2$ (**42**), and OCH_2Ph (**47**), can markedly improve the activity against *Escherichia coli*. For electron-withdrawing group NO_2 , F, and Br, the activity gradient of substituent group on the phenyl ring in *p*-position is $\text{NO}_2 > \text{F} > \text{Br}$ which accords with their ability of withdrawing electron. However, when NO_2 , F, and Br moiety is in *o*-position, the ability against *E. coli* decreases almost simultaneously. Compound **40** with two different halogen groups on the *o*-position manifested higher antibacterial activity with IC_{50} value of $82 \mu\text{g}/\text{mL}$ against *E. coli* than compounds **37**, **38** and **44** with only one halogen moiety. On the contrary, compound **41**, two same halogen groups on the phenyl ring, performed inferior antibacterial activity. In comparison, we found that the derivatives which have electron-withdrawing substituents (such as F, Cl, Br) and bulky group on the benzene ring exhibited more potent antibacterial activities than those have electron-donating substituents (such as CH_3 , OCH_3). We proposed that, for these compounds, electron-withdrawing and bulky groups were conducive to the antibacterial activity and compounds with electron-donating halogen groups were not favorable for activity.

2.2.2. *E. coli* FabH and *P. aeruginosa* FabH inhibitory activity

The *E. coli* FabH and *P. aeruginosa* FabH inhibitory potency of the selected compound **30**, **33**, **36–38** and **46–47** was examined and

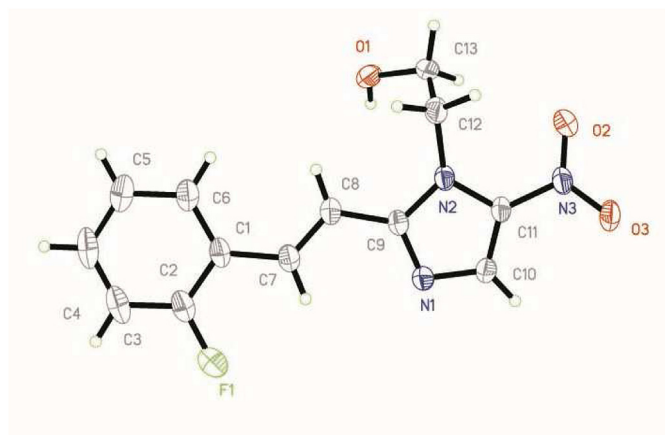


Fig. 2. Crystal structure diagram of compound **37**. H atoms are shown as small spheres of arbitrary radii.

Table 2
Crystallographical and experimental data for compounds **35** and **37**.

Compound	35	37
Empirical formula	$\text{C}_{13}\text{H}_{12}\text{BrN}_3\text{O}_3$	$\text{C}_{13}\text{H}_{12}\text{FN}_3\text{O}_3$
Formula weight	338.21	277.12
Crystal system	Monoclinic	Monoclinic
Space group	<i>P</i> <i>c</i>	<i>P</i> <i>c</i>
<i>a</i> (Å)	7.6657 (8)	7.5690 (5)
<i>b</i> (Å)	8.7493 (9)	7.9036 (5)
<i>c</i> (Å)	10.4323 (11)	10.8599 (7)
α (°)	83.093 (3)	87.613 (2)
β (°)	73.977 (3)	82.578 (2)
γ (°)	84.711(3)	85.173(2)
<i>V</i> (Å ³)	666.35(12)	641.63(7)
<i>Z</i>	8	11
<i>D</i> _{calc} /g cm ⁻³	2.451	1.766
<i>h</i> range (°)	2.04–25.86	3.11–27.52
<i>F</i> (000)	456	341
Reflections collected	5720 (<i>R</i> _{int} = 0.0305)	6790 (<i>R</i> _{int} = 0.0198)
Data/restraints/parameters	2562/0/182	2863/0/182
Absorption coefficient (mm ⁻¹)	12.083	0.198
<i>R</i> ₁ ; <i>wR</i> ₂ [<i>I</i> > 2σ(<i>I</i>)]	0.0406/0.1027	0.0435/0.1179
<i>R</i> ₁ ; <i>wR</i> ₂ (all data)	0.0580/0.1112	0.0550/0.1281
GO _F	1.021	1.033

the results were summarized in Table 4. As shown in Table 4, among the tested compounds, compounds **33** and **47**, displaying the most potent *E. coli* inhibitory activity, showed potent inhibitory activities with IC_{50} of 2.1 and 3.4 μM , respectively, which were comparable to the positive control Kanamycin with IC_{50} of 3.1 μM . Compound **30**, as the most promising anti-*P. aeruginosa* agent with IC_{50} of 1.7 μM (Table 3), showed low *P. aeruginosa* FabH inhibitory activity with IC_{50} of 22.5 μM . In contrast, compounds **46** and **47**, which exhibited average *P. aeruginosa* inhibitory activity, showed more strong inhibitory effect and its 50% *P. aeruginosa* FabH inhibition concentration of 7.9 and 10.2 μM . This may imply that the potent inhibitory

Table 3
Antibacterial activities of synthetic compounds.

Compound	50% inhibitory concentrations ($\mu\text{g}/\text{mL}$)			
	Gram-negative		Gram-positive	
	<i>Escherichia coli</i>	<i>Pseudomonas aeruginosa</i>	<i>Bacillus thuringiensis</i>	<i>Bacillus subtilis</i>
25	>200	12.4 ± 0.44	49.5 ± 0.13	49.3 ± 0.43
26	89.1 ± 6.09	30.2 ± 0.34	67.4 ± 0.32	146.4 ± 0.14
27	119.3 ± 4.22	32.2 ± 0.23	19.2 ± 0.42	113.5 ± 0.51
28	114.1 ± 3.05	16.8 ± 0.13	55.1 ± 0.74	36.6 ± 0.65
29	>200	48.3 ± 0.89	32.1 ± 0.34	32.8 ± 0.67
30	57.2 ± 2.39	1.7 ± 0.64	12.5 ± 0.78	8.8 ± 0.45
31	119.1 ± 15.24	14.7 ± 0.23	25.7 ± 0.29	40.7 ± 0.43
32	>200	46.1 ± 0.13	12.1 ± 0.43	26.2 ± 0.10
33	36.4 ± 2.33	15.5 ± 0.54	13.9 ± 0.55	9.0 ± 0.33
34	187.8 ± 9.65	20.4 ± 0.16	37.3 ± 0.60	19.8 ± 0.43
35	115.8 ± 8.44	43.6 ± 0.75	23.4 ± 0.71	24.4 ± 0.56
36	59.2 ± 0.37	70.3 ± 0.03	5.9 ± 0.63	17.9 ± 0.47
37	>200	6.8 ± 0.13	29.9 ± 0.66	61.5 ± 0.23
38	174.7 ± 0.78	17.8 ± 0.43	37.8 ± 0.54	2.9 ± 0.13
39	144.8 ± 10.22	2.9 ± 0.17	28.6 ± 0.41	42.6 ± 0.13
40	82.1 ± 9.90	38.1 ± 0.19	25.3 ± 0.34	19.6 ± 0.17
41	>200	39.3 ± 0.45	36.7 ± 0.40	57.1 ± 0.12
42	88 ± 5.03	120.9 ± 0.44	7.2 ± 0.71	17.2 ± 0.45
43	>200	74.6 ± 0.32	7.0 ± 0.22	53.1 ± 0.21
44	>200	7.6 ± 0.27	9.3 ± 0.27	27.9 ± 0.13
45	157.2 ± 8.23	12.8 ± 0.40	5.8 ± 0.42	11.8 ± 0.10
46	>200	19.8 ± 0.54	11.9 ± 0.90	3.6 ± 0.50
47	34.3 ± 4.46	14.5 ± 0.17	9.8 ± 0.24	6.3 ± 0.53
48	153.4 ± 6.31	13.1 ± 0.30	8.6 ± 0.23	13.6 ± 0.34
Kanamycin	47.3 ± 7.83	6.8 ± 0.13	9.5 ± 0.25	8.9 ± 0.73
Penicillamine	42.3 ± 3.91	5.8 ± 0.19	6.3 ± 0.72	6.3 ± 0.43

Table 4
E. coli FabH and *P. aeruginosa* FabH inhibitory activities of selected compounds.

Compound	<i>E. coli</i> FabH IC ₅₀ (μM)	<i>P. aeruginosa</i> FabH IC ₅₀ (μM)
30	16.5	22.5
33	2.1	12.4
36	4.2	15.9
37	4.4	19.2
38	6.5	29.2
42	10.2	25.6
46	11.0	10.2
47	3.4	7.9
Kanamycin	3.1	6.7

effects of the synthetic compounds against *P. aeruginosa* may not correlated to *P. aeruginosa* FabH, and this result complied with the new research from different groups [28–30]. Other tested compounds displayed moderate inhibitory activities with IC₅₀ ranging from 4.2 to 16.5 μM against *E. coli* FabH. It suggested that the modifications in the 2-methyl group of metronidazole were favorable for the FabH inhibitory activity. We can also conclude from our observed activity results that the compound which showed good docking energies against *E. coli* FabH and good IC₅₀ against *E. coli* FabH, should not necessarily that they show good antibacterial activities against *E. coli*.

2.2.3. Cytotoxicity

As compounds **33** and **47** exhibited potent antimicrobial activity, their detailed toxicological studies on human macrophage were carried out. As showed in Figs. 3 and 4, the MTT assay revealed that the viability of macrophage was inversely proportional to the concentration of the compounds **33** and **47**. Further more, after cultured for 24 h, Morphological anomalies in macrophage exposed to different concentration compound **33** (0.25, 160 μg/mL) showed nothing different from morphological in control under phase contrast microscope (Figs. 5–7). It recommended that both compounds **33** and **47** did not exhibit any toxicity towards morphological.

2.2.4. Binding model of compounds 33, 47 and *E. coli* FabH

Molecular docking of the synthesized compounds and *E. coli* FabH was performed on the binding model based on the *E. coli* FabH–CoA complex structure (1HNJ.pdb) [31]. The coordinate of

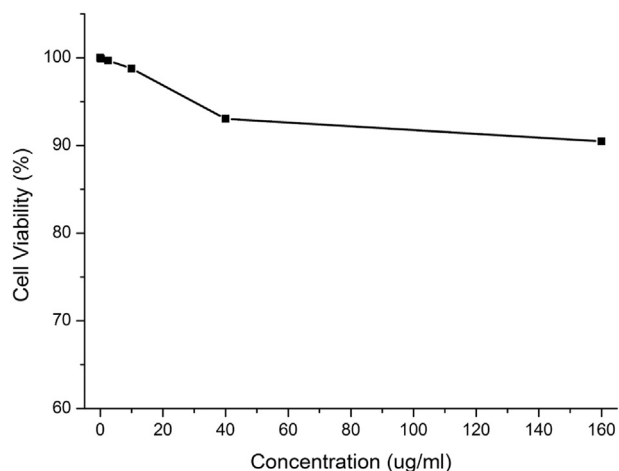


Fig. 3. Viability (determined by MTT assay) of macrophage exposed to compound **33** after 24 h.

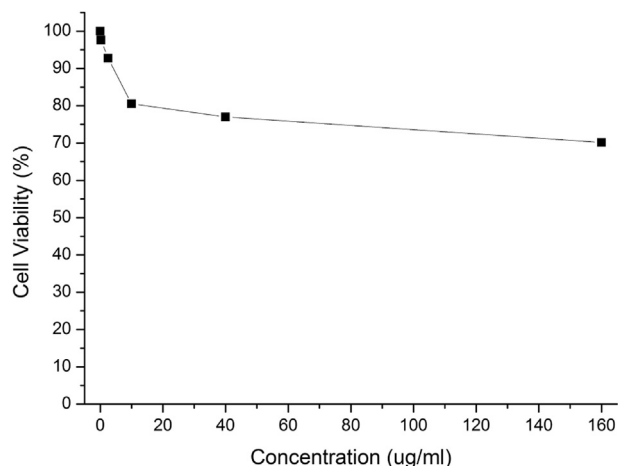


Fig. 4. Viability (determined by MTT assay) of macrophage exposed to compound **47** after 24 h.



Fig. 5. Morphological changes in macrophage at 0.25 μg/mL of compound **33**.

the input site sphere is 28.4494, 9.90349, 33.4428 and the radius of the sphere is 11 Å.

All docking runs were applied Ligand Fit Dock protocol of Discovery Studio 3.1. The binding model of compounds **33**, **47** and

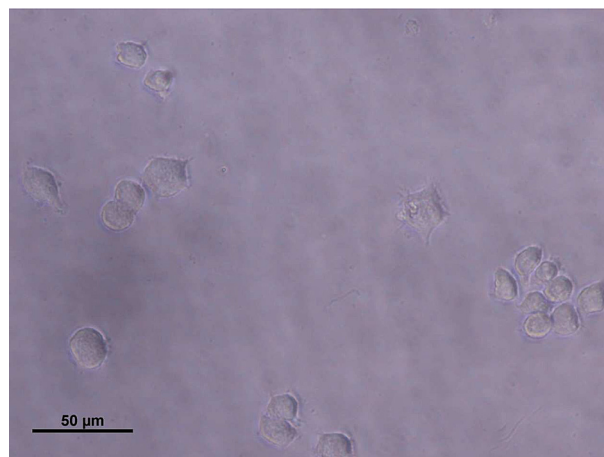


Fig. 6. Morphological changes in macrophage at 160 μg/mL of compound **33**.



Fig. 7. Normal growth of macrophage (control).

E. coli FabH was depicted in Figs. 8 and 9. The amino acid residues which had interaction with FabH as well as bond length were labeled. In the binding mode, compound **33** was nicely bound to FabH via three hydrogen bonds with Met207 (angle O–H–N = 141.6°, distance = 2.33 Å), Asn247 (angle O–H–N = 124.5°, distance = 2.34 Å and angle O–H–N = 137.4°, distance = 2.30 Å), six charge interactions and one π – π interaction. The end group of Arg249, Arg46 and Asp150 were respectively formed six charge

interactions with two nitro group, which were accordant exactly with the previous work of FabH inhibitors. Meanwhile, the nitrogen atom of nitro group formed a π – π interaction with Phe213. As for compound **47**, it also performed a nice bonding situation via three hydrogen bonds together with two π –cation interactions. This ensured the binding affinity and results in an increased FabH inhibitory activity. Arg219 and Arg56 formed two remarkable π –cation interactions with two benzene rings respectively. Besides, the hydrogen of Asn274, Asn274 and Arg56 were formed three hydrogen bonds interaction with oxygen atom of nitro group of compound **47** (angle O–H–N = 131.1°, distance = 2.10 Å), nitrogen atom of pyrazol group of compound **47** (angle N–H–N = 147.9°, distance = 2.40 Å) and oxygen atom linking two benzene rings of compound **47** (angle N–H–N = 101.8°, distance = 2.60 Å) each other. This molecular docking result, along with the biological assay data, suggested that compounds **33** and **47** were a potential inhibitor of FabH. The docking calculation of all the compounds was also depicted in Table 5. The CDocker Energy (energy of the ligand–receptor complexes) agreed with the FabH inhibitory trend for all the synthesized compounds.

3. Conclusion

To conclude, a series of novel 2-styryl 5-nitroimidazole derivatives **25–48** were synthesized through straightforward chemistry and tested for their inhibitory activities against *E. coli*, *P. aeruginosa*, *B. subtilis* and *B. thuringiensis*. Most of them exhibited

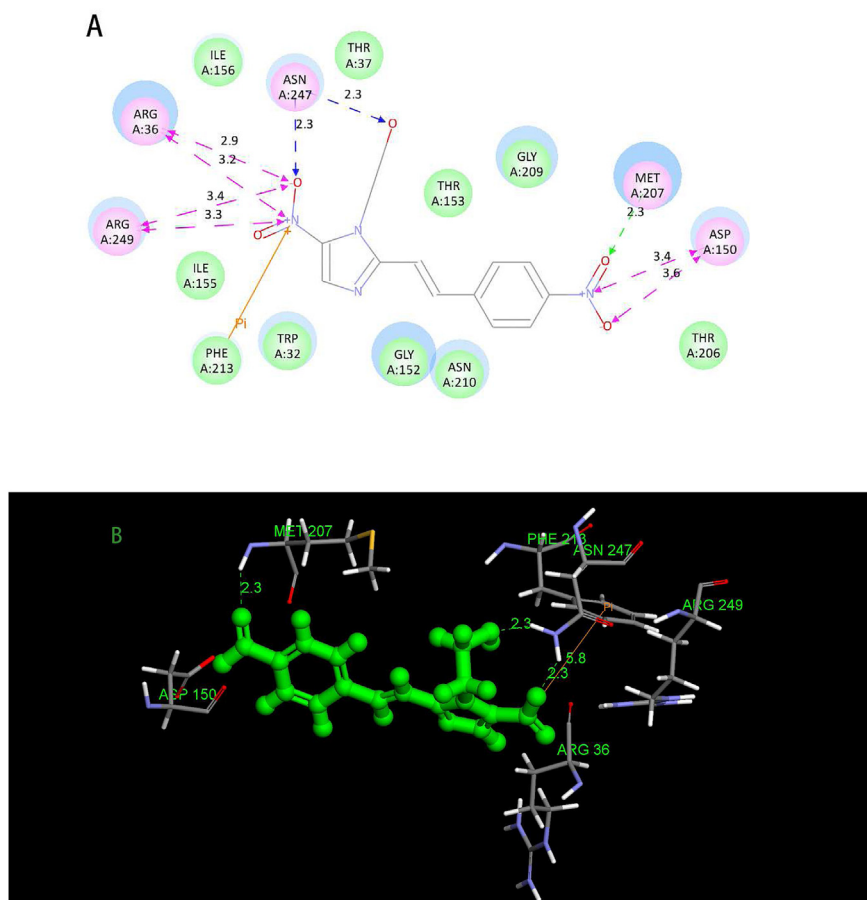


Fig. 8. (A) 2D model of the interaction between compound **33** and *E. coli* FabH. π -cation bond is displayed as orange lines. H-bonds are displayed as blue and green dashed lines. (B) 3D model of the interaction between compound **33** and *E. coli* FabH. (For interpretation of the references to color in this figure legend, the reader is referred to the web version of this article.)

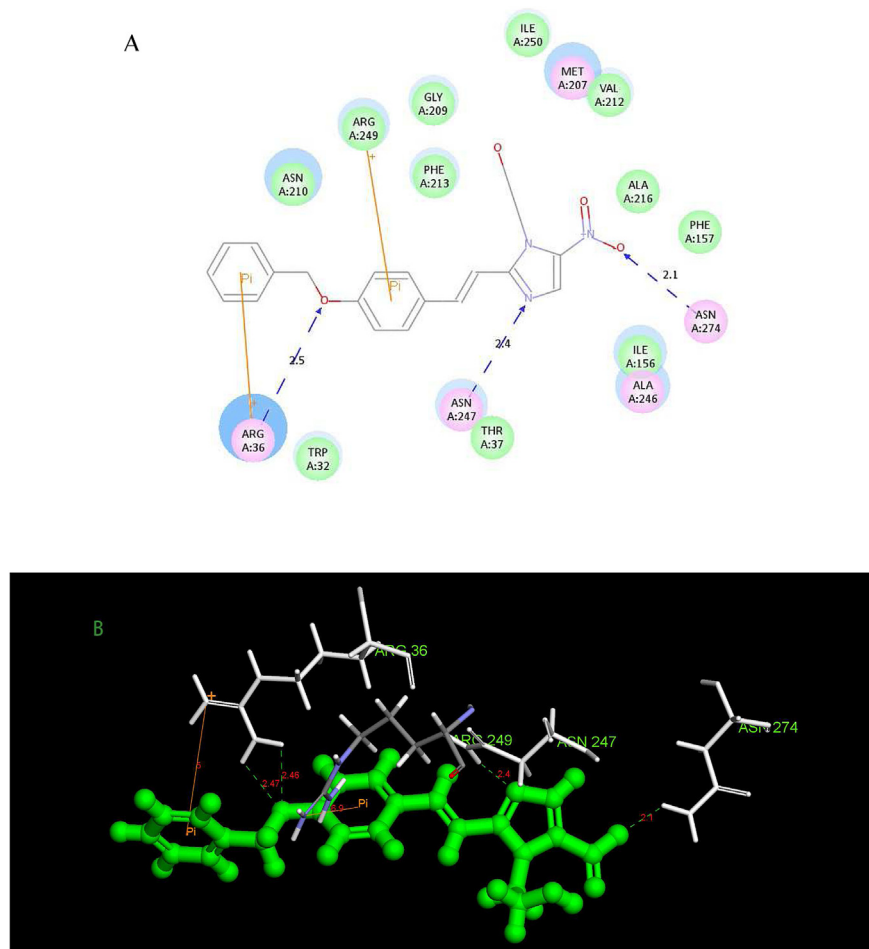


Fig. 9. (A) 2D model of the interaction between compound **47** and *E. coli* FabH. P-cation bonds are displayed as orange lines. H-bonds are displayed as blue and green dashed lines. (B) 3D model of the interaction between compound **47** and *E. coli* FabH. (For interpretation of the references to color in this figure legend, the reader is referred to the web version of this article.)

potent antibacterial and *E. coli* FabH inhibitory activities. Compounds **33** and **47** showed the most potent FabH inhibition activities ($IC_{50} = 2.1, 3.1 \mu\text{M}$) and antimicrobial activities ($IC_{50} = 33.0, 34.3 \mu\text{g/mL}$ for *E. coli*, $IC_{50} = 15.5, 14.5 \mu\text{g/mL}$ for *P. aeruginosa*, $IC_{50} = 13.9, 9.8 \mu\text{g/mL}$ for *B. thuringiensis* and $IC_{50} = 9.0, 6.3 \mu\text{g/mL}$ for *B. subtilis*), and more, did not show any toxicity towards morphological. The docking simulation was performed to get the probable binding models and poses. The results indicated that compounds **33** and **47**, which acted as potential FabH inhibitors, can both bind well into the active site of FabH. The result of this work

might be helpful for the design and synthesis of FabH inhibitors with stronger activities.

4. Experiments

4.1. Materials and measurements

All chemicals used were purchased from Aldrich (USA). Melting points (uncorrected) were determined on a X-4 MP apparatus (Taik Corp, Beijing, China). All the ^1H NMR spectra were recorded on a Bruker DPX 300 model Spectrometer in $\text{DMSO}-d_6$ and chemical shifts were reported in ppm (δ). Elemental analyses were performed on a CHN–O–Rapid instrument and were within $\pm 0.4\%$ of the theoretical values. ESI-MS spectra were recorded on a Mariner System 5304 Mass spectrometer.

4.2. General method of synthesis of metronidazole derivatives

Reaction of metronidazole (12 mmol) with different substituted benzaldehyde (16 mmol) in 6 mL DMSO by adding rapidly a stirred solution of sodium methoxide (12.8 mmol) in methanol at room temperature resulted in the formation of target compounds.

4.2.1. 2-(5-Nitro-2-styryl-1H-imidazol-1-yl)ethanol(**25**)

Yield 83.1%; M.p. 75–78 °C. ^1H NMR ($\text{DMSO}-d_6$, 300 MHz) δ : 8.22 (s, 1H, CH), 7.79–7.61 (m, 2H, ArH), 7.52 (d, $J = 7.6$ Hz, 1H, CH), 7.51–

Table 5
The docking calculation of the synthesized compounds.

Compound	CDocker Energy Δ Gb (kcal/mol)	Compound	CDocker Energy Δ Gb (kcal/mol)
25	–22.34	37	–30.01
26	–21.23	38	–29.60
27	–15.34	39	–18.83
28	–28.22	40	–15.27
29	–23.12	41	–28.65
30	–19.89	42	–25.32
31	–13.13	43	–21.47
32	–25.23	44	–20.26
33	–35.54	45	–27.76
34	–31.12	46	–20.33
35	–23.56	47	–33.17
36	–31.75	48	–31.08

7.40 (m, 3H, ArH), 7.30–7.19 (m, 1H, CH), 4.96 (s, 1H, OH), 4.61 (t, $J = 5.1$ Hz, 2H, CH₂), 3.70 (m, 2H, CH₂). ESI-MS: 260.10 (C₁₃H₁₄N₃O₃, [M+H]⁺). Anal. Calcd for C₁₃H₁₃N₃O₃: C, 60.22; H, 5.05; N, 16.21. Found: C, 57.12; H, 5.03; N, 16.15.

4.2.2. 2-(2-(4-Methoxystyryl)-5-nitro-1H-imidazol-1-yl)ethanol(**26**)

Yield 74.5%; M.p. 82–85 °C. ¹H NMR (DMSO-*d*₆, 300 MHz) δ : 8.12 (s, 1H, CH), 7.71–7.11 (m, 4H, ArH), 6.93 (d, $J = 5.4$ Hz, 2H, CH), 4.93 (s, 1H, OH), 4.55 (t, $J = 5.1$ Hz, 2H, CH₂), 3.73 (t, $J = 6.3$ Hz, 2H, CH₂), 1.13 (s, 3H, CH₃). ESI-MS: 290.11 (C₁₄H₁₆N₃O₄, [M+H]⁺). Anal. Calcd for C₁₄H₁₅N₃O₄: C, 58.13; H, 5.23; N, 14.53. Found: C, 59.12; H, 5.20; N, 15.04.

4.2.3. 2-(2-(4-Bromostyryl)-5-nitro-1H-imidazol-1-yl)ethanol(**27**)

Yield 77.0%; M.p. 76–79 °C. ¹H NMR (DMSO-*d*₆, 300 MHz) δ : 8.22 (d, $J = 6.8$ Hz, 1H, CH), 7.97–7.78 (m, 3H, ArH), 7.54–7.39 (m, 3H, ArH, CH), 5.01 (t, $J = 4.5$ Hz, 1H, OH), 4.70 (t, $J = 6.0$ Hz, 2H, CH₂), 3.72–3.65 (m, 2H, CH₂). ESI-MS: 238.01 (C₁₃H₁₃BrN₃O₃, [M+H]⁺). Anal. Calcd for C₁₃H₁₂BrN₃O₃: C, 46.17; H, 3.58; N, 12.43. Found: C, 44.58; H, 3.54; N, 12.07.

4.2.4. 2-(2-(3-Fluorostyryl)-5-nitro-1H-imidazol-1-yl)ethanol(**28**)

Yield 76.4%. M.p. 75–77 °C. ¹H NMR (DMSO-*d*₆, 300 MHz) δ : 8.21 (s, 1H, CH), 7.79–7.69 (m, 2H, ArH), 7.57 (d, $J = 7.7$ Hz, 1H, CH), 7.51–7.42 (m, 2H, ArH), 7.24–7.18 (m, 1H, CH), 4.99 (s, 1H, OH), 4.65 (t, $J = 5.1$ Hz, 2H, CH₂), 3.71 (m, 2H, CH₂). ESI-MS: 278.09 (C₁₃H₁₃FN₃O₃, [M+H]⁺). Anal. Calcd for C₁₃H₁₂FN₃O₃: C, 56.32; H, 4.36; N, 15.16. Found: C, 43.24; H, 4.38; N, 13.59.

4.2.5. 2-(2-(4-Chlorostyryl)-5-nitro-1H-imidazol-1-yl)ethanol(**29**)

Yield 68.3%. M.p. 76–78 °C. ¹H NMR (DMSO-*d*₆, 300 MHz) δ : 8.23 (d, $J = 5.0$ Hz, 1H, CH), 7.89–7.65 (m, 3H, ArH), 7.43–7.27 (m, 3H, ArH, CH), 5.04–4.95 (m, 1H, OH), 4.70–4.54 (m, 2H, CH₂), 3.86–3.65 (m, 2H, CH₂). ESI-MS: 294.06 (C₁₃H₁₃ClN₃O₃, [M+H]⁺). Anal. Calcd for C₁₃H₁₂ClN₃O₃: C, 53.16; H, 4.12; N, 14.31. Found: C, 48.57; H, 4.09; N, 15.23.

4.2.6. 2-(2-(4-Fluorostyryl)-5-nitro-1H-imidazol-1-yl)ethanol(**30**)

Yield 73.2%. M.p. 77–80 °C. ¹H NMR (DMSO-*d*₆, 300 MHz) δ : 8.22 (d, $J = 4.7$ Hz, 1H, CH), 7.86–7.75 (m, 3H, ArH), 7.39–7.25 (m, 3H, ArH, CH), 5.04–4.97 (m, 1H, OH), 4.64–4.49 (m, 2H, CH₂), 3.73–3.68 (m, 2H, CH₂). ESI-MS: 278.09 (C₁₃H₁₃FN₃O₃, [M+H]⁺). Anal. Calcd for C₁₃H₁₂FN₃O₃: C, 56.32; H, 4.36; N, 15.16. Found: C, 47.68; H, 4.37; N, 16.63.

4.2.7. 2-(2-(3-Chlorostyryl)-5-nitro-1H-imidazol-1-yl)ethanol(**31**)

Yield 69.7%. M.p. 75–78 °C. ¹H NMR (DMSO-*d*₆, 300 MHz) δ : 8.22 (s, 1H, CH), 7.83–7.69 (m, 3H, ArH), 7.57–7.36 (m, 3H, ArH, CH), 5.02 (t, $J = 3.7$ Hz, 1H, OH), 4.34 (t, $J = 6.0$ Hz, 2H, CH₂), 3.62–3.49 (m, 2H, CH₂). ESI-MS: 294.06 (C₁₃H₁₃ClN₃O₃, [M+H]⁺). Anal. Calcd for C₁₃H₁₂ClN₃O₃: C, 53.16; H, 4.12; N, 14.31. Found: C, 38.69; H, 4.10; N, 14.92.

4.2.8. 2-(2-(2-Methoxystyryl)-5-nitro-1H-imidazol-1-yl)ethanol(**32**)

Yield 73.2%; M.p. 79–82 °C. ¹H NMR (DMSO-*d*₆, 300 MHz) δ : 8.22 (s, 1H, CH), 7.76–7.65 (m, 1H, CH), 7.60–7.44 (m, 4H, ArH), 6.83 (d, $J = 6.0$ Hz, 1H, CH), 5.02 (s, 1H, OH), 4.62–4.50 (m, 2H, CH₂), 3.71 (t, $J = 6.2$ Hz, 2H, CH₂), 1.14 (s, 3H, CH₃). ESI-MS: 290.11 (C₁₄H₁₆N₃O₄, [M+H]⁺). Anal. Calcd for C₁₄H₁₅N₃O₄: C, 58.13; H, 5.23; N, 14.53. Found: C, 47.54; H, 5.20; N, 13.91.

4.2.9. 2-(2-(4-Nitrostyryl)-5-nitro-1H-imidazol-1-yl)ethanol(**33**)

Yield 73.1%. M.p. 79–83 °C. ¹H NMR (DMSO-*d*₆, 300 MHz) δ : 8.29–8.20 (m, 4H, ArH, CH), 8.05–7.87 (m, 2H, ArH), 7.61 (d, $J = 15.8$ Hz, 1H, CH), 5.01 (t, $J = 5.6$ Hz, 1H, OH), 4.8 (t, $J = 5.0$ Hz, 2H, CH₂), 3.75–3.70 (m, 2H, CH₂). ESI-MS: 305.08 (C₁₃H₁₃N₄O₅, [M+H]⁺). Anal. Calcd for C₁₃H₁₂N₄O₅: C, 51.32; H, 3.98; N, 18.41. Found: C, 50.71; H, 3.96; N, 16.37.

4.2.10. 2-(2-(3-Methoxystyryl)-5-nitro-1H-imidazol-1-yl)ethanol(**34**)

Yield 68.1%; M.p. 80–82 °C. ¹H NMR (DMSO-*d*₆, 300 MHz) δ : 8.15 (s, 1H, CH), 7.81–7.43 (m, 4H, ArH), 6.93 (d, $J = 6.4$ Hz, 2H, CH), 5.01 (s, 1H, OH), 4.53 (t, $J = 5.6$ Hz, 2H, CH₂), 3.79 (m, 2H, CH₂), 1.18 (s, 3H, CH₃). ESI-MS: 290.11 (C₁₄H₁₆N₃O₄, [M+H]⁺). Anal. Calcd for C₁₄H₁₅N₃O₄: C, 58.13; H, 5.23; N, 14.53. Found: C, 50.17; H, 5.21; N, 16.01.

4.2.11. 2-(2-(3-bromostyryl)-5-nitro-1H-imidazol-1-yl)ethanol(**35**)

Yield 64.8%. M.p. 81–83 °C. ¹H NMR (DMSO-*d*₆, 300 MHz) δ : 8.22 (s, 1H, CH), 8.08 (s, 1H, ArH), 7.76–7.71 (m, 2H, ArH), 7.57–7.36 (m, 3H, ArH, CH), 4.99 (t, $J = 4.0$ Hz, 1H, OH), 4.65 (t, $J = 5.7$, 2H, CH₂), 3.73–3.68 (m, 2H, CH₂). ESI-MS: 238.01 (C₁₃H₁₃BrN₃O₃, [M+H]⁺). Anal. Calcd for C₁₃H₁₂BrN₃O₃: C, 46.17; H, 3.58; N, 12.43. Found: C, 43.75; H, 3.55; N, 12.13.

4.2.12. 2-(2-(4-(Dimethoxymethyl)styryl)-5-nitro-1H-imidazol-1-yl)ethanol(**36**)

Yield 76.5%. M.p. 83–86 °C. ¹H NMR (DMSO-*d*₆, 300 MHz) δ : 8.00 (s, 1H, CH), 7.67–7.41 (m, 4H, ArH), 6.57 (t, $J = 7.14$ Hz, 2H, CH₂), 4.80 (t, $J = 5.6$ Hz, 1H, OH), 4.40 (t, $J = 6.0$ Hz, 2H, CH₂), 3.75–3.50 (m, 6H, CH₂), 1.21–1.10 (m, 6H, CH₃). ESI-MS: 362.16 (C₁₈H₂₄N₃O₅, [M+H]⁺). Anal. Calcd for C₁₈H₂₃N₃O₅: C, 59.82; H, 6.41; N, 11.63. Found: C, 54.73; H, 6.38; N, 11.58.

4.2.13. 2-(2-(2-Fluorostyryl)-5-nitro-1H-imidazol-1-yl)ethanol(**37**)

Yield 69.2%. M.p. 77–80 °C. ¹H NMR (DMSO-*d*₆, 300 MHz) δ : 8.22 (d, $J = 4.74$, 1H, CH), 7.82–7.70 (m, 3H, ArH), 7.64 (d, $J = 5.4$ Hz, 1H, CH), 7.42–7.30 (m, 2H, ArH, CH), 5.15–4.94 (m, 1H, OH), 4.54 (t, $J = 8.4$ Hz, 2H, CH₂), 3.77–3.70 (m, 2H, CH₂). ESI-MS: 278.09 (C₁₃H₁₃FN₃O₃, [M+H]⁺). Anal. Calcd for C₁₃H₁₂FN₃O₃: C, 56.32; H, 4.36; N, 15.16. Found: C, 54.20; H, 4.34; N, 14.78.

4.2.14. 2-(2-(2-Chlorostyryl)-5-nitro-1H-imidazol-1-yl)ethanol(**38**)

Yield 71%. M.p. 74–77 °C. ¹H NMR (DMSO-*d*₆, 300 MHz) δ : 8.20 (s, 1H, CH), 7.85–7.72 (m, 3H, ArH), 7.61–7.32 (m, 3H, ArH, CH), 5.00 (t, $J = 5.4$ Hz, 1H, OH), 4.50 (t, $J = 6.7$ Hz, 2H, CH₂), 3.65 (m, 2H, CH₂). ESI-MS: 294.06 (C₁₃H₁₃ClN₃O₃, [M+H]⁺). Anal. Calcd for C₁₃H₁₂ClN₃O₃: C, 53.16; H, 4.12; N, 14.31. Found: C, 49.54; H, 4.09; N, 13.67.

4.2.15. 2-(2-(4-Methylstyryl)-5-nitro-1H-imidazol-1-yl)ethanol(**39**)

Yield 65.3%; M.p. 82–85 °C. ¹H NMR (DMSO-*d*₆, 300 MHz) δ : 7.94 (s, 1H, CH), 7.81–7.62 (m, 4H, ArH), 7.44 (d, $J = 7.9$ Hz, 2H, CH), 4.86 (s, 1H, OH), 4.35 (t, $J = 6.4$ Hz, 2H, CH₂), 3.63 (t, $J = 7.2$ Hz, 2H, CH₂), 1.22 (s, 3H, CH₃). ESI-MS: 290.11 (C₁₄H₁₆N₃O₃, [M+H]⁺). Anal. Calcd for C₁₄H₁₅N₃O₃: C, 61.53; H, 5.53; N, 15.38. Found: C, 57.43; H, 5.49; N, 16.25.

4.2.16. 2-(2-(2-chloro-6-fluorostyryl)-5-nitro-1H-imidazol-1-yl)ethanol(**40**)

Yield 72.5%. M.p. 86–88 °C. ¹H NMR (DMSO-*d*₆, 300 MHz) δ : 8.05 (s, 1H, CH), 7.67–7.38 (m, 4H, ArH, CH), 6.78 (d, $J = 5.4$ Hz, 1H, CH), 4.97 (t, $J = 5.6$ Hz, 1H, OH), 4.35 (t, $J = 6.0$ Hz, 2H, CH₂), 3.68–3.53 (m, 6H, CH₂). ESI-MS: 314.06 (C₁₃H₁₄ClFN₃O₃, [M+H]⁺). Anal.

Calcd for $C_{13}H_{13}ClFN_3O_3$: C, 49.77; H, 4.18; N, 13.39. Found: C, 48.38; H, 4.14; N, 12.27.

4.2.17. 2-(2-(2,4-Dichlorostyryl)-5-nitro-1H-imidazol-1-yl)ethanol(**41**)

Yield 69.5%. M.p. 85–88 °C; 1H NMR (DMSO- d_6 , 300 MHz) δ : 8.00 (s, 1H, CH), 7.65–7.43 (m, 2H, ArH), 7.37–7.20 (m, 2H, ArH, CH), 6.94 (d, $J = 8.5$ Hz, H, CH), 4.57 (t, $J = 6.1$ Hz, 1H, OH), 4.38 (t, $J = 9.6$ Hz, 2H, CH_2), 3.72–3.57 (m, 2H, CH_2). ESI-MS: 330.03 ($C_{13}H_{14}Cl_2N_3O_3$, $[M+H]^+$). Anal. Calcd for $C_{13}H_{13}Cl_2N_3O_3$: C, 47.29; H, 3.97; N, 12.73. Found: C, 45.35; H, 3.95; N, 12.53.

4.2.18. 2-(2-(4-Dimethylaminostyryl)-5-nitro-1H-imidazol-1-yl)ethanol (**42**)

Yield 68.4%. M.p. 86–88 °C; 1H NMR (DMSO- d_6 , 300 MHz) δ : 8.06 (s, 1H, CH), 7.83–7.70 (m, 2H, ArH), 7.00–6.73 (m, 2H, ArH), 6.97 (t, $J = 6.7$ Hz, 2H, CH), 5.00 (t, $J = 6.2$ Hz, 1H, OH), 4.37 (t, $J = 7.4$ Hz, 2H, CH_2), 3.68–3.53 (m, 2H, CH_2), 1.46–1.19 (m, 6H, CH_3). ESI-MS: 305.15 ($C_{15}H_{19}N_4O_3$, $[M+H]^+$). Anal. Calcd for $C_{15}H_{18}N_4O_3$: C, 59.59; H, 6.00; N, 18.53. Found: C, 43.87; H, 6.03; N, 17.73.

4.2.19. 2-(2-(3-Nitrostyryl)-5-nitro-1H-imidazol-1-yl)ethanol(**43**)

Yield 74.1%. M.p. 81–82 °C; 1H NMR (DMSO- d_6 , 300 MHz) δ : 8.31–7.73 (m, 3H, ArH, CH), 7.70–7.54 (m, 2H, ArH), 7.35–7.16 (m, 2H, CH), 4.85 (t, $J = 7.3$ Hz, 1H, OH), 4.53 (t, $J = 6.4$ Hz, 2H, CH_2), 3.65 (m, 2H, CH_2). ESI-MS: 305.08 ($C_{13}H_{13}N_4O_5$, $[M+H]^+$). Anal. Calcd for $C_{13}H_{12}N_4O_5$: C, 50.98; H, 4.61; N, 18.29. Found: C, 47.87; H, 4.57; N, 17.53.

4.2.20. 2-(2-(3-Bromostyryl)-5-nitro-1H-imidazol-1-yl)ethanol(**44**)

Yield 68.6%. M.p. 79–82 °C; 1H NMR (DMSO- d_6 , 300 MHz) δ : 8.22 (d, $J = 4.74$, 1H, CH), 7.86–7.75 (m, 3H, ArH), 7.39–7.25 (m, 3H, ArH, CH), 5.04–4.97 (m, 1H, OH), 4.64–4.49 (m, 2H, CH_2), 3.73–3.68 (m, 2H, CH_2). ESI-MS: 238.01 ($C_{13}H_{13}BrN_3O_3$, $[M+H]^+$). Anal. Calcd for $C_{13}H_{12}BrN_3O_3$: C, 46.17; H, 3.58; N, 12.43. Found: C, 38.94; H, 3.56; N, 11.75.

4.2.21. 2-(2-(2-Nitrostyryl)-5-nitro-1H-imidazol-1-yl)ethanol(**45**)

Yield 72.1%. M.p. 77–80 °C; 1H NMR (DMSO- d_6 , 300 MHz) δ : 8.25 (d, $J = 6.73$ Hz, 1H, CH), 8.03–7.94 (m, 3H, ArH, CH), 7.83–7.58 (m, 3H, ArH, CH), 4.99 (t, $J = 6.3$ Hz, 1H, OH), 4.54 (t, $J = 5.4$ Hz, 2H, CH_2), 3.74–3.52 (m, 2H, CH_2). ESI-MS: 305.08 ($C_{13}H_{13}N_4O_5$, $[M+H]^+$). Anal. Calcd for $C_{13}H_{12}N_4O_5$: C, 51.32; H, 3.98; N, 18.41. Found: C, 49.26; H, 3.94; N, 16.54.

4.2.22. 2-(2-(2-(Naphthalen-2-yl)vinyl)-5-nitro-1H-imidazol-1-yl)ethanol (**46**)

Yield 71.4%. M.p. 86–89 °C; 1H NMR (DMSO- d_6 , 300 MHz) δ : 8.05–7.92 (m, 3H, ArH, CH), 7.89–7.64 (m, 2H, ArH), 7.61 (t, $J = 6.5$ Hz, 2H, ArH), 7.43 (t, $J = 7.3$ Hz, 1H, ArH), 7.09–6.87 (m, 2H, CH), 5.02 (t, $J = 7.6$ Hz, 1H, OH), 4.41 (t, $J = 6.0$ Hz, 2H, CH_2), 3.70–3.58 (m, 2H, CH_2). ESI-MS: 310.11 ($C_{17}H_{16}N_3O_3$, $[M+H]^+$). Anal. Calcd for $C_{17}H_{15}N_3O_3$: C, 66.01; H, 4.89; N, 13.58. Found: C, 57.89; H, 4.86; N, 14.25.

4.2.23. 2-(2-(4-(Benzyloxy)styryl)-5-nitro-1H-imidazol-1-yl)ethanol(**47**)

Yield 72.3%. M.p. 84–87 °C; 1H NMR (DMSO- d_6 , 300 MHz) δ : 7.99 (d, $J = 5.8$ Hz, 1H, CH), 7.64–7.50 (m, 4H, ArH), 7.42–7.26 (m, 3H, ArH), 7.08–6.90 (m, 4H, Ar, CH), 5.16 (t, $J = 5.1$ Hz, 2H, CH_2), 4.54 (t, $J = 6.7$ Hz, 1H, OH), 4.39 (t, $J = 8.3$ Hz, 2H, CH_2), 3.68–3.54 (m, 2H, CH_2). ESI-MS: 366.14 ($C_{20}H_{21}N_3O_4$, $[M+H]^+$). Anal. Calcd for $C_{20}H_{19}N_3O_4$: C, 65.74; H, 5.24; N, 11.50. Found: C, 63.83; H, 5.23; N, 12.98.

4.2.24. 2-(2-(2-(Naphthalen-1-yl)vinyl)-5-nitro-1H-imidazol-1-yl)ethanol (**48**)

Yield 75.7%. M.p. 86–89 °C; 1H NMR (DMSO- d_6 , 300 MHz) δ : 8.16–7.93 (m, 4H, ArH, CH), 7.76–7.43 (m, 4H, ArH), 6.63 (t, $J = 4.3$ Hz, 2H, CH_2), 4.81 (t, $J = 6.9$ Hz, 1H, OH), 4.30 (t, $J = 5.1$ Hz, 2H, CH_2), 3.70 (m, 2H, CH_2). ESI-MS: 310.11 ($C_{17}H_{16}N_3O_3$, $[M+H]^+$). Anal. Calcd for $C_{17}H_{15}N_3O_3$: C, 66.01; H, 4.89; N, 13.58. Found: C, 64.29; H, 4.88; N, 12.91.

4.3. Crystal structure determination

Crystal structure determination of compounds **35** and **37** were carried out on Bruker SMARTAPEX CCD diffractometer at 293(2) K using Mo K_α radiation ($\lambda = 0.71073\text{\AA}$) by the ω scan mode. The structure was solved by direct methods and refined on F^2 by full-matrix least-squares methods using SHELX-97. All the non-hydrogen atoms were refined anisotropically. All the hydrogen atoms were placed in calculated positions and were assigned fixed isotropic thermal parameters at 1.2 times the equivalent isotropic U of the atoms to which they are attached and allowed to ride on their respective parent atoms. The contributions of these hydrogen atoms were included in the structure factors calculations. The crystal data, data collection and refinement parameters for the compound **35** and **37** were listed in Table 2.

4.4. Antibacterial activity

The antibacterial activity of the synthesized compounds was tested against *E. coli*, *B. thuringiensis*, *B. subtilis* and *P. aeruginosa* using MH medium (Mueller–Hinton medium: casein hydrolyzate 17.5 g, soluble starch 1.5 g, beef extract 1000 mL). Seed 104 bacteria per well into 96-well plates, incubate at 37 °C for 24 h. Then add 100 μ L a series concentration of drug-containing medium into wells to maintain the final concentration of drug as 320, 160, 40, 10, 2.5 and 0.25 μ g/mL. One concentration should be triplicated. After 12 h, bacterial survival was determined by the addition of an MTT (3-(4,5-dimethylthiazol-2-yl)-2,5-diphenyl tetrazolium bromide) solution (25 mL of 5 mg/mL MTT in PBS). After 4 h, discard the medium and add 150 μ L DMSO. The plates were voted for 10 min to make completely dissolution. Optical absorbance was measured at 490 nm.

4.5. *E. coli* FabH purification and activity assay

Full-length *E. coli* ACP, acyl carrier protein synthase (ACPS), and FabH were individually cloned into pET30 expression vectors with an N-terminal His-tag.

All proteins were expressed in *E. coli* strain BL21 (DE3). Transformed cells were grown on Luria–Bertani (LB) agar plates supplemented with kanamycin (30 μ g/mL). Sodium dodecyl sulfate–polyacrylamide gel electrophoresis (SDS–PAGE) analysis was used to screen colonies for overexpression of proteins. One such positive colony was used to inoculate 10 mL of LB medium with 30 μ g/mL of kanamycin and grown overnight at 37 °C, 1 mL of which was used to inoculate 100 mL LB medium supplemented with 30 mg/mL of kanamycin. The culture was shaken for 4 h at 37 °C, and then induced with 0.5 mM isopropyl β -D-thiogalactopyranoside (IPTG). The culture was grown for 4 h, and harvested by centrifugation (30 min at 15,000 rpm).

Harvested cells containing FabH were lysed by sonication in 20 mM Tris, pH 7.6, 5 mM imidazole, 0.5 M NaCl and centrifuged at 20,000 rpm for 30 min. The supernatant was applied to a Ni-NTA agarose column, washed, and eluted using a 5–500 mM imidazole gradient over 20 column volumes. Eluted protein was dialyzed against 20 mM Tris, pH 7.6, 1 mM DTT, and 100 mM NaCl.

Purified FabD and FabHs were concentrated up to 2 mg/mL and stored at -80°C in 20 mM Tris, pH 7.6, 100 mM NaCl, 1 mM DTT, and 20% glycerol for enzymatic assay.

Purified ACP contains the apo-form that needs to be converted into the holo-form. The conversion reaction is catalyzed by ACP synthase (ACPS). In the final volume of 50 mL, 50 mg ACP, 50 mM Tris, 2 mM DTT, 10 mM MgCl_2 , 600 μM CoA, and 0.2 μM ACPS was incubated for 1 h at 37°C . The pH of the reaction was then adjusted to approximately 7.0 using 1 M potassium phosphate. Holo-ACP was purified by fractionation of the reaction mixture by Source Q-15 ion exchange chromatography using a 0–500 mM NaCl gradient over 25 column volumes.

In a final 20 μL reaction, 20 mM Na_2HPO_4 , pH 7.0, 0.5 mM DTT, 0.25 mM MgCl_2 , and 2.5 μM holo-ACP were mixed with 1 nM FabH, and H_2O was added to 15 μL . After 1 min incubation, a 2 μL mixture of 25 μM acetyl-CoA, 0.5 mM NADH, and 0.5 mM NADPH was added for FabH reaction for 25 min. The reaction was stopped by adding 20 μL of ice-cold 50% TCA, incubating for 5 min on ice, and centrifuging to pellet the protein. The pellet was washed with 10% ice-cold TCA and resuspended with 5 μL of 0.5 M NaOH. The incorporation of the 3H signal in the final product was read by liquid scintillation. When determining the inhibition constant (IC_{50}), inhibitors were added from a concentrated DMSO stock such that the final concentration of DMSO did not exceed 2%.

4.6. Cytotoxicity

To test the toxicity of compounds **6a** and **6f** against mammalian cells, human macrophage was used. The cell was grown in DMEM medium supplemented with 10% FBS and $1\times$ antimycotic and antibacterial solution (Sigma USA) at 37°C , in humidified atmosphere having 5% CO_2 . One hundred microliters of the confluent fibroblast stock suspension was dispensed in 96-well tissue culture plate. The original medium from the wells was replaced with 100 μL serum free DMEM when the cells reached 90% confluency after 5 h incubation in a CO_2 incubator. Various concentrations of the test compounds (160, 40, 10, 2.5, 0.25 $\mu\text{g}/\text{mL}$) were added to the growing cells and incubated for 24 h. Response of cells to the test compounds was determined spectrophotometrically at 570 and 630 nm. The difference between absorbance at 570 and 630 nm was used as an index of the cell viability. The morphology of the cells was observed using Giemsa stain under Phase contrast microscope [32].

4.7. Docking simulations

Molecular docking of compounds into the three-dimensional X-ray structure of FabH was carried out using CDOCKER Dock protocol of Discovery Studio 3.1.

Acknowledgments

We thank Miss Zhu Shen in Nanjing Foreign Languages School for the synthesis of compounds 37 and 38 of this paper. This work was supported by Major Projects on Control and Rectification of Water Body Pollution (No. 2011ZX07204-001-004), and was supported by 'PCSIRT' (IRT1020).

Appendix A. Supplementary data

Supplementary data related to this article can be found at <http://dx.doi.org/10.1016/j.ejmech.2014.02.004>.

References

- [1] P. Gastmeier, D. Sohr, C. Geffers, M. Behnke, F. Daschner, H. Rüdén, Mortality risk factors with nosocomial *Staphylococcus aureus* infections in intensive care units: results from the German Nosocomial Infection Surveillance System (KISS), *Infection* 33 (2005) 50–55.
- [2] V. Varshney, N.N. Mishra, P.K. Shukla, D.P. Sahu, Synthesis of nitroimidazole derived oxazolidinones as antibacterial agents, *European Journal of Medicinal Chemistry* 45 (2010) 661–666.
- [3] P. Zhan, X. Liu, Y. Cao, Y. Wang, C. Pannecouque, E.D. Clercq, 1,2,3-Thiadiazole thioacetanilides as a novel class of potent HIV-1 non-nucleoside reverse transcriptase inhibitors, *Bioorganic & Medicinal Chemistry Letters* 18 (2008) 5368–5371.
- [4] A.R. Bhat, Tazeem, A. Amir, I. Choi, F. Athar, 3-(1,3,4-Thiadiazole-2-yl) quinoline derivatives. Synthesis, characterization and antimicrobial activity, *European Journal of Medicinal Chemistry* 46 (2011) 3158–3166.
- [5] L. Otvos Jr., J.D. Wade, F. Lin, B.A. Condie, J. Hanrieder, R. Hoffmann, Designer antibacterial peptides kill fluoroquinolone-resistant clinical isolates, *Journal of Medicinal Chemistry* 48 (2005) 5349–5359.
- [6] Z.L. Li, Q.S. Li, H.J. Zhang, Y. Hu, D.D. Zhu, H.L. Zhu, Design, synthesis and biological evaluation of urea derivatives from *o*-hydroxybenzylamines and phenylisocyanate as potential FabH inhibitors, *Bioorganic & Medicinal Chemistry* 19 (2011) 4413–4420.
- [7] Y. Cui, Y. Dang, Y. Yang, S. Zhang, Syntheses and antibacterial activity of a series of 3-(pyridine-3-yl)-2-oxazolidinone, *European Journal of Medicinal Chemistry* 40 (2005) 209–214.
- [8] Y. Li, Y. Luo, Y. Hu, D.D. Zhu, S. Zhang, Z.J. Liu, H.L. Gong, H.L. Zhu, Design, synthesis and antimicrobial activities of nitroimidazole derivatives containing 1,3,4-oxadiazole scaffold as FabH inhibitors, *Bioorganic & Medicinal Chemistry* 20 (2012) 4316–4322.
- [9] N. Tabanca, E. Bedir, N. Kirimer, K.H.C. Baser, S.I. Khan, M.R. Jacob, I.A. Khan, Antimicrobial compounds from *pimpinella* species growing in Turkey, *Planta Medica* 69 (2003) 933–938.
- [10] N.S. Survay, B. Kumar, M. Jang, D.Y. Yoon, Y.S. Jung, D.C. Yang, S.W. Park, Two novel bioactive glucosinolates from Broccoli (*Brassica oleracea* L. var. *italica*) florets, *Bioorganic & Medicinal Chemistry Letters* 22 (2012) 5555–5558.
- [11] R.K. Pettit, G.R. Pettit, E. Hamel, F. Hogan, B.R. Moser, S. Wolf, S. Pon, J.C. Chapuis, J.M. Schmidt, E -Combretastatin and E -resveratrol structural modifications: antimicrobial and cancer cell growth inhibitory β -E-nitrostyrenes, *Bioorganic & Medicinal Chemistry* 17 (2009) 6606–6612.
- [12] J.S. Solanki, T.R. Thapak, A. Bhardwaj, U.N. Tripathi, Synthesis, structural characterization, and in vitro antimicrobial properties of salicylate and pyrazoline complexes of bismuth(III), *Journal of Coordination Chemistry* 64 (2011) 369–376.
- [13] J.Y. Lee, K.W. Jeong, J.U. Lee, D.I. Kang, Y. Kim, Antimicrobial natural products as β -ketoacyl-acyl carrier protein synthase III inhibitors, *Bioorganic & Medicinal Chemistry* 17 (2009) 5408–5413.
- [14] H.J. Zhang, Z.L. Li, H.L. Zhu, Advances in the research of β -ketoacyl-ACP synthase III (FabH) inhibitors, *Current Medicinal Chemistry* 19 (2012) 1225–1237.
- [15] J.Y. Lee, K.W. Jeong, J.U. Lee, D.I. Kang, Y. Kim, Novel *E. coli* β -ketoacyl-acyl carrier protein synthase III inhibitors as targeted antibiotics, *Bioorganic & Medicinal Chemistry* 17 (2009) 1506–1513.
- [16] S.S. Khandekar, R.A. Daines, J.T. Lonsdale, Bacterial β -ketoacyl-acyl carrier protein synthases as targets for antibacterial agents, *Current Protein & Peptide Science* 4 (2003) 21–29.
- [17] R.J. Heath, C.O. Rock, The claisen condensation in biology, *Natural Product Reports* 19 (2002) 581–596.
- [18] C.E. Christensen, B.B. Kragelund, W.K.P. Von, A. Henriksen, Structure of the human β -ketoacyl [ACP] synthase from the mitochondrial type II fatty acid synthase, *Protein Science* 16 (2007) 261–272.
- [19] M. Abid, M. Subhash, Agarwal, A. Azam, Synthesis and antimicrobial activity of metronidazole thiosemicarbazone analogues, *European Journal of Medicinal Chemistry* 43 (2008) 2035–2039.
- [20] A.C. Wassmann, E. Hellberg, I. Tannich, Bruchhaus, Metronidazole resistance in the protozoan parasite *Entamoeba histolytica* is associated with increased expression of iron-containing superoxide dismutase and peroxiredoxin and decreased expression of ferredoxin 1 and flavin reductase, *Journal of Biological Chemistry* 274 (1999) 26051–26056.
- [21] R. Siles, S.E. Chen, M. Zhou, K.G. Pinney, M.L. Trawick, Design, synthesis, and biochemical evaluation of novel cruzain inhibitors with potential application in the treatment of Chagas' disease, *Bioorganic & Medicinal Chemistry Letters* 16 (2006) 4405–4409.
- [22] Y. Luo, K.M. Qiu, X. Lu, J. Fu, H.L. Zhu, Metronidazole acid acyl sulfonamide: a novel class of anticancer agents and potential EGFR tyrosine kinase inhibitors, *Bioorganic & Medicinal Chemistry* 19 (2011) 6069–6076.
- [23] H.J. Zhang, Y. Qian, K. Liu, D.D. Zhu, J. Zhao, X.M. Wang, H.L. Zhu, Synthesis, antibacterial activities and molecular docking studies of Schiff bases derived from *N*-(2/4-benzaldehyde-amino) phenyl-*N'*-phenyl-thiourea, *Bioorganic & Medicinal Chemistry* 19 (2011) 5708–5715.
- [24] D. Olender, J. Zwawiak, L. Zaprutko, Synthesis of some *N*-substituted nitroimidazole derivatives as potential antioxidant and antifungal agents, *European Journal of Medicinal Chemistry* 44 (2009) 645–652.

- [25] J.A. Upcroft, L.A. Dunn, J.M. Wright, K. Benakli, P. Upcroft, et al., 5-nitroimidazole drugs effective against metronidazole-resistant *Trichomonas vaginalis* and *Giardia duodenalis*, *Antimicrobial Agents and Chemotherapy* 50 (2006) 344–347.
- [26] J.A. Upcroft, R.W. Campbell, K. Benakli, P. Upcroft, P. Vanelle, Efficacy of new 5-nitroimidazoles against metronidazole-susceptible and -resistant *Giardia*, *Trichomonas*, and *Entamoeba* spp., *Antimicrobial Agents and Chemotherapy* 43 (1999) 73–76.
- [27] D.I. Edwards, Mechanism of antimicrobial action of metronidazole, *Journal of Antimicrobial Chemotherapy* 5 (1979) 499–502.
- [28] Y.-M. Zhang, C.O. Rock, Will the initiator of fatty acid synthesis in *Pseudomonas aeruginosa* please stand up? *Journal of Bacteriology* 194 (2012) 5159–5161.
- [29] Y. Yuan, M. Sachdeva, J.A. Leeds, T.C. Meredith, Fatty acid biosynthesis in *Pseudomonas aeruginosa* is initiated by the FabY class of β -ketoacyl acyl carrier protein synthases, *Journal of Bacteriology* 194 (2012) 5171–5184.
- [30] Y. Yuan, J.A. Leeds, T.C. Meredith, *Pseudomonas aeruginosa* directly shunts β -oxidation degradation intermediates into de novo fatty acid biosynthesis, *Journal of Bacteriology* 194 (2012) 5185–5196.
- [31] X. Qiu, C.A. Janson, W.W. Smith, M. Head, J. Lonsdale, A.K. Refined Konstantinidis, Structures of β -ketoacyl-acyl carrier protein synthase III, *Journal of Molecular Biology* 307 (2001) 341–356.
- [32] H.Q. Li, Li Shi, Q.S. Li, P.G. Liu, Y. Luo, J. Zhao, H.L. Zhu, Synthesis of C(7) modified chrysin derivatives designing to inhibit beta-ketoacyl-acyl carrier protein synthase III (FabH) as antibiotics, *Bioorganic & Medicinal Chemistry* 17 (2009) 6264–6269.